Exploration of Supercritical Condition in the Los Humeros Geothermal Field

Eva Schill[1], Natalia Cornejo-Triviño[2] and Domenico Liotta[3]

[1]Lawrence Berkeley National Laboratory, 1 Cyclotron Road, 94720 Berkeley, California, USA

[2]Technical University Darmstadt, Schnittspahnstraße 9, 64287 Darmstadt, Germany

[3]Dipartimento di Scienze della Terra e Geoambientali, Via Edoardo Orabona, 4, 70125 Bari, BA, Italy

eschill@lbl.gov

Keywords: Los Humeros geothermal fields, sub- and supercritical resources, gravity, fluid chemistry

ABSTRACT

Sub- and supercritical geothermal resources offer significantly higher energy densities than conventional hydrothermal systems, primarily due to the low viscosity and high enthalpy of supercritical fluids, which can substantially increase the thermal output per well. These fluids may form through conductive heating and boiling of groundwater near magmatic intrusions and are chemically distinct—typically exhibiting low concentrations of rock-forming elements and elevated levels of volatiles such as carbon, sulfur, and boron. Their chemical signatures are governed by the solubility of salts, oxides, and aluminum silicates in high-temperature, low-density fluids (Heřmanská et al., 2020).

Despite their potential, identifying sub- to supercritical resources remains challenging. Laboratory experiments have shown that electrical conductivity increases from 25 °C to about 350 °C due to enhanced surface and electrolytic conduction but drops significantly under supercritical conditions (374–600 °C) as water density and dielectric properties decrease (Nono et al., 2020). At temperatures between 500–700 °C, the conductivity of most crustal rocks approaches that of dry rocks.

At the Los Humeros geothermal field, analysis of temperature and fluid chemistry data suggests the presence of sub- to supercritical conditions in the northern sector of the reservoir. To explore geophysical signatures associated with these conditions, we analyzed gravity and magnetotelluric inversion results over the relevant subsurface volume. While both methods revealed anomalies consistent in scale with the expected sub- to supercritical fluid-bearing zones, no clear correlation with the temperature and fluid chemistry indicators was observed. However, the spatial alignment of these indicators with the direction of gravity anomalies that have been attributed to characterize the tectonic influence on the geothermal field (Cornejo-Triviño et al., 2024) is striking.

1. INTRODUCTION

Sub- and supercritical geothermal resources offer significantly higher energy densities compared to conventional hydrothermal systems. Due to their low viscosity and high enthalpy, supercritical fluids can transport substantially more thermal energy, potentially increasing the energy output per well by up to an order of magnitude. Supercritical fluids with temperatures in the range of 400-500 °C have been reported in several active geothermal fields worldwide (Heřmanská et al., 2020). Geochemical experiments and modeling indicate that such fluids can form through conductive heating and boiling of subcritical geothermal groundwater in the presence of a magmatic intrusion. As such, they are characterized by low concentrations of mineral-forming elements such as Si, Na, K, Ca, Mg, and Al. These concentrations are governed by the solubility of salts, oxides, and aluminum silicates in high-temperature (T > 400 °C), low-density (ρ < 300 kg/m³) fluids. In contrast, these fluids tend to exhibit elevated concentrations of volatile elements (e.g., C, S, B) of crustal and/or mantle origin. Interestingly, the concentrations of these volatiles are often comparable to those found in subcritical geothermal fluids.

However, accurately identifying and distinguishing these high-temperature resources from conventional hydrothermal systems remains a major exploration and characterization challenge. Joint interpretation of electrical resistivity and gravity data has become standard in hydrothermal exploration, as each method is sensitive to different physical properties—resistivity to fluids and alteration, gravity to density contrasts and structure. Joint inversion can reduce the inherent non-uniqueness of individual methods by enforcing structural or petrophysical links between models. At the Sorik Marapi field (Sumatra), a 3D joint inversion of magnetotelluric and gravity data, incorporating fault discontinuities, improved delineation of the graben structure. Gravity resolved lateral geometry, while magnetotelluric provided depth resolution (Soyer et al., 2020). In Los Humeros (Mexico), combining gravity and surface-wave dispersion data led to better-constrained velocity and density models than from separate inversions (Carrillo et al., 2024). Nevertheless, some studies opt for so-called cooperative joint inversion approaches, such as cross-gradient or structure-coupled constraints, which offer a flexible alternative (Um et al., 2023).

In the Los Humeros geothermal field, gravity data do not directly delineate the geothermal reservoir; rather, they provide a robust framework for understanding the subsurface structure and help constrain the uncertainty of the geological model (Cornejo-Triviño et al., subm.). Its 3-D resistivity model, derived from magnetotelluric data inversion, reveals a classic geothermal signature characterized by a dome-shaped low-resistivity clay cap overlying a more resistive core (Benediktsdóttir et al., 2019). The resistivity distribution shows a strong correlation with faults and seismicity, highlighting the structurally controlled permeability of the geothermal reservoir.

Recent laboratory experiments at temperatures ranging from 25 °C to about 350 °C, electrical conductivity increases because of both increasing surface and electrolytic conduction (Nono et al., 2020). Under supercritical conditions, i.e. temperature from 374 °C to 600 °C, electrical conductivity strongly decreases due to the evolution of water density and dielectric constant that affect both surface and electrolyte conduction. Apart from amphibolite, crustal rock conductivities at temperatures between 500 °C and 700 °C lie within the range of dry rock electrical conductivity values.

With the aim of identifying geophysical signatures associated with sub- to supercritical temperatures, this study, compares gravity and electric resistivity of the Los Humeros geothermal field. The Los Humeros geothermal field is situated in the northeastern part of the Trans-Mexican Volcanic Belt. Los Humeros hosts several wells with temperatures that suggest the potential presence of supercritical fluids (Figure 1). While gravity data help delineate key structural features, electrical resistivity is used to characterize thermally relevant zones. Our interpretations are benchmarked against temperature measurements reported by Espinosa-Paredes & Garcia-Gutierrez (2003).

2. LITHOLOGY AND THERMAL STRUCTURE OF THE LOS HUMEROS GEOTHERMAL FIELD

The Los Humeros geothermal field is characterized by Mesozoic sedimentary rocks of the Sierra Madre Oriental, locally metamorphosed to marble, hornfels, and skarn near intrusions of syenitic to granitic plutons (Yáñez-García & García-Durán, 1982). The overlying volcanic succession is divided into pre-caldera, caldera, and post-caldera units. The pre-caldera group (up to about 1,500 m thick) includes basaltic to andesitic lavas of the Teziutlán Formation (2.6-1.4 Ma), older basaltic flows, and Cuyoaco Formation lavas (8.9-10.5 Ma), along with localized basaltic to rhyolitic lavas and domes (270-693 ka; Carrasco-Núñez et al., 2018, 2022). The caldera group includes the Xáltipan ignimbrite (164 ka), a thick pyroclastic unit (90-780 m) with porosity up to 70% (Cavazos-Álvarez et al., 2020), overlain by the Faby Tuff (70 ka) and the Zaragoza ignimbrite (69 ka), which formed the nested Los Potreros caldera (Carrasco-Núñez et al., 2018, 2022). The post-caldera group consists of Late Pleistocene rhyolitic to dacitic lavas and pyroclastics, followed by Holocene explosive and effusive volcanism. Amphibole crystals occur in the hottest parts of the geothermal system, in the Colapso Central area at depths of > 1,600 m (Martínez-Serrano, 2002).

The static formation temperatures (Figure 2a) estimated for the Los Humeros geothermal field (Espinosa-Paredes & Garcia-Gutierrez, 2003) indicate a high potential for the presence of supercritical fluids. Notably, deep wells exceeding about 2,000 m in the central to northern sectors of the field show maximum values that surpass the critical temperature of water, suggesting favorable conditions for supercritical geothermal resources. Note that Espinosa-Paredes & Garcia-Gutierrez (2003), applying a spherical radial flow model for temperature correction, suggest temperatures above the critical point in nine wells (H-8, H-11, H-12, H-20, H-26-29, H-32).

Mineral-forming element concentrations in the Los Humeros fluids are low while the concentrations of gases like CO_2 and H_2S are high (Heřmanská et al., 2020). Based on water isotopes (δD and $\delta 18O$, Figure 2a), the source fluids are dominantly meteoric (Lelli et al., 2021). The concentrations of boron in the fluids reach up to > 1000 ppm (Bernard et al. 2011, Figure 2b). The isotope values of the volatile elements suggest a magmatic contribution with $\delta 11B$ of -0.8‰ and $\delta 13C-CO_2$ of -3.5‰ (Bernard, 2008).

The content of total dissolved solids in the Los Humeros fluids decreases with temperature (Espinosa-Paredes & Garcia-Gutierrez, 2003, Figure 2c). These observations point to supercritical fluids formed by conductive heating and boiling of about 200-300°C subcritical geothermal water with their concentrations controlled by the solubility of salts, oxides, and aluminum silicates in high-temperature (400 °C) and low-density (ρ_b of 300 kg m^{-3}) water as suggested by Heřmanská et al. (2020).

Based on the evaluation of corrected temperature data (T > 350 °C) and fluid chemistry, specifically boron concentrations exceeding C_{Boron} > 1,000 ppm, we anticipate the reasonable presence of subcritical to supercritical fluids in the central part of the study area (Figure 1). Notably, temperatures above 350 °C are typically recorded at depths around 2,200 m, whereas elevated boron concentrations at lower temperatures are observed in wells at approximately 1,700 m depth.
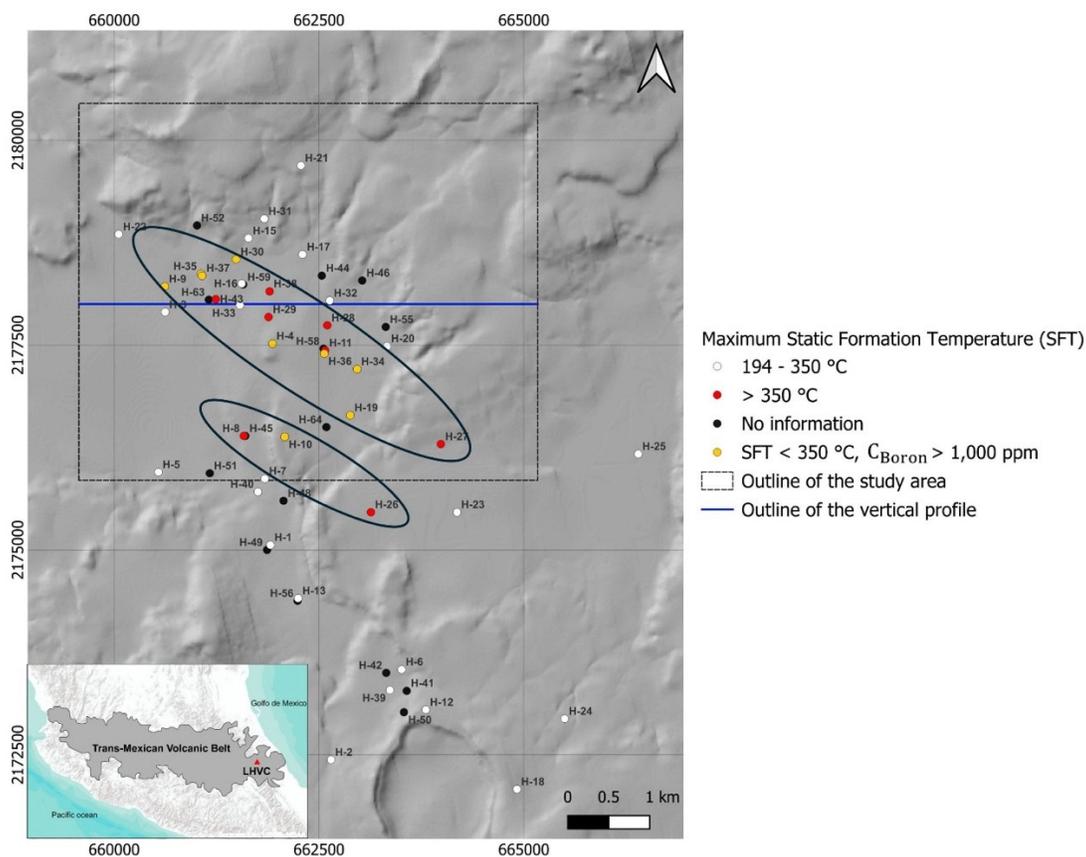
Figure 1: Distribution of wells and maximum static formation temperatures after Horner (1951) in the Los Humeros geothermal field (Espinosa-Paredes & Garcia-Gutierrez, 2003) or with mean boron concentrations CBoron > 1,000 ppm (data from Tello, 2005; Diez, 2015; Heřmanská et al., 2020). The black ellipsoids outline of the expected sub- to supercritical fluid extend based on the temperatures and confirmed by high boron concentrations. The blue line shows the position of the representative gravity and electric resistivity E-W profiles in Figure 3. Inset map shows the location of the Los Humeros geothermal field within the Trans-Mexican Volcanic Belt.
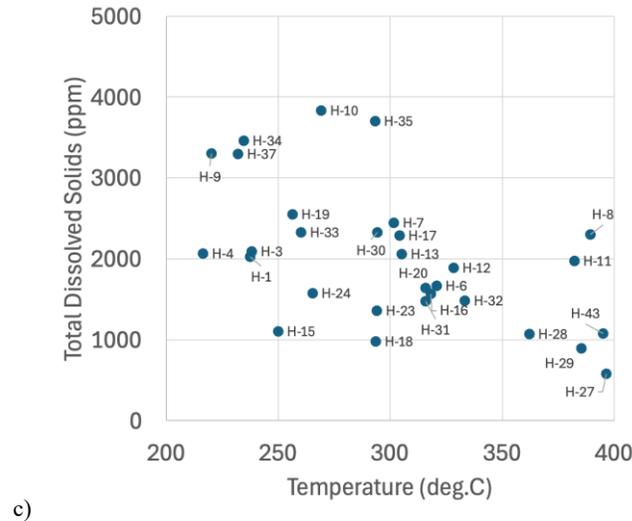
c)
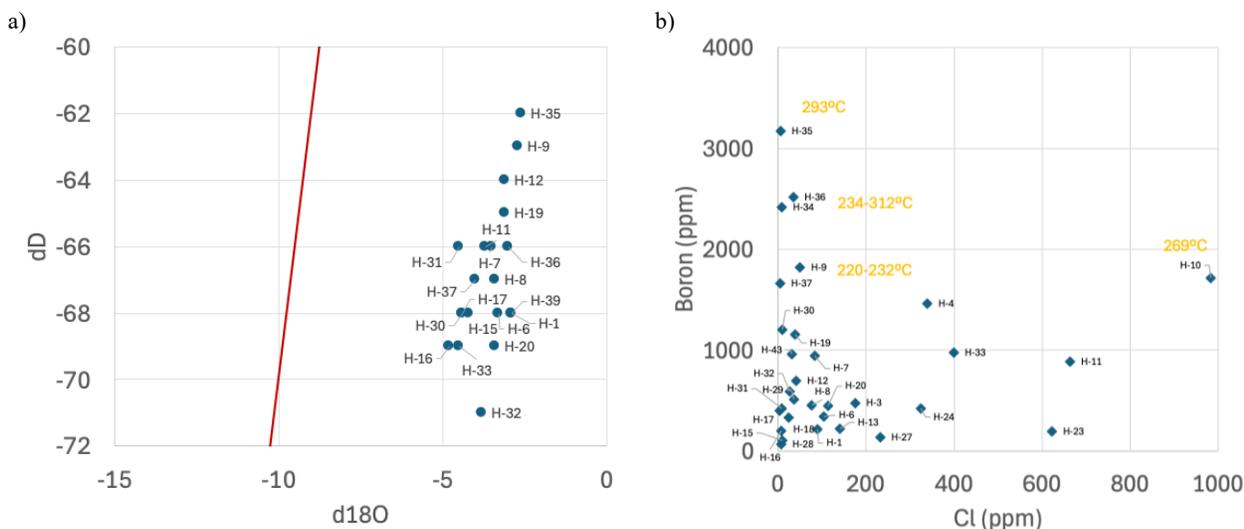
Figure 2: a) Total fluid isotope (after Hinojosa 2005) determined in the Los Humeros wells in comparison to the Global Meteoric Water Line (GMWL, after Craig 1961). b) Boron versus chloride concentrations. Orange number indicate the maximum static formation Horner-temperature after Espinosa-Paredes & Garcia-Gutierrez (2003). c) Total dissolved solids determined as a function of maximum static formation Horner-temperature after Espinosa-Paredes & Garcia-Gutierrez (2003).

3. GEOPHYSICAL DATA OF THE LOS HUMEROS GEOTHERMAL FIELD

Gravity data were acquired at 263 stations along ten east–west profiles across the central and northern Los Humeros geothermal field (Figure 1). Data acquisition and processing procedures are described in Cornejo-Triviño et al. (2024).

The processed residual gravity anomaly was analyzed through both forward and inverse modeling (Cornejo-Triviño et al., subm.), constrained by the 3-D geological model of Calcagno et al. (2022). The structural framework was discretized into 17,388 voxels (200 × 200 × 100 m). Multiple density parameterizations were tested to refine the models. Inversion using a Markov Chain Monte Carlo stochastic algorithm implemented in GeoModeller (Intrepid Geophysics) showed that including compaction and porosity corrections achieved the best match with observations. The optimal inversion was obtained with a 70 % probability of density changes and a 30 % probability of geometry changes, confirming that the initial 3-D geological model is largely consistent with the observed gravity field.

Magnetotelluric and transient electromagnetic data were collected across the Los Humeros geothermal field, consisting of 122 magnetotelluric soundings and 120 co-located TEM stations distributed throughout the area. Details of data acquisition, processing, and static-shift correction are provided in Benediktsdóttir et al. (2019).

A 3-D resistivity model of Los Humeros was developed using WSINV3DMT (Siripunvaraporn et al., 2005; Siripunvaraporn & Egbert, 2009). The inversion incorporated smoothness constraints and a prior model as regularization parameters, following a stepwise iterative approach to progressively improve the data fit. Several starting models were evaluated, and the final model, initiated from a homogeneous 50 Ωm half-space, was selected for its ability to reproduce a geologically plausible and parsimonious resistivity structure, minimizing artifacts observed in alternative runs.

4. RESULTS AND DISCUSSION

The temperature and fluid chemistry data of the potential sub- to supercritical fluid-bearing zones is summarized in Table 1. Figure 1 shows the spatial distribution of the key wells that provide evidence for these conditions. Notably, these wells are arranged along two distinct, approximately NE–SW trending structural corridors.

Table 1: Selected wells with maximum static formation temperatures after Horner (1951) in the Los Humeros geothermal field (Espinosa-Paredes & Garcia-Gutierrez, 2003) and mean boron concentrations (data from Tello, 2005; Diez et al., 2015; Heřmanská et al., 2020).

Well	Depth (meters)	Maximum Static Formation Temperature (°C)	Boron Concentraion (ppm)
H-4	1,855	216.5	1,127
H-8	2,300	389.4	453

4

H-9	2,300	220.2	1,822
H-10	2,158	269.2	1,716
H-11	2,376	382.1	882
H-19	2,269	256.3	1,155
H-26	2,546	364.5	
H-27	2,584	396.4	135
H-28	2,558	362.1	67
H-29	2,186	385.3	513
H-30	1,902	294.3	1,202
H-34	1,760	234.6	2,417
H-35	1,680	293.2	3,170
H-36	1,698	312.3	2,516
H-37	1,670	232.1	1,660
H-38	2,190	353.6	
H-43	2,200	395	958

To identify resistivity or density anomalies potentially associated with sub- to supercritical conditions, we examine the 3-D inversions of subsurface volume beginning at 1,200 m a.s.l. (Figure 3), which corresponds to the average depth of wells exhibiting elevated boron concentrations of about 1,700 m. This depth interval provides a relevant reference for correlating geophysical signatures with geochemical evidence of high-temperature fluid presence. While the density inversion primarily reflects the geological setting of the study area (Figure 3a; Cornejo-Triviño et al., subm.), the 3D resistivity model (Benediktsdóttir et al., 2019) reveals deep few hundreds of meter-scale anomalies that cut across the stratigraphy and structural fabric. Beginning at depths greater than 2,200 m, the resistivity data show distinct low-conductivity anomalies in the eastern and western parts of the study area. These are separated by a more conductive zone centrally located, forming a prominent resistivity contrast across the field (Figure 3b).

At 1,200 m a.s.l., which corresponds to the average depth of wells with elevated boron concentrations, these anomalies span approximately 200 meters in thickness and extend 1,000 to 2,000 meters in the north–south direction (Figure 3d). Notably, within the basement rock, where density becomes laterally homogeneous (Figure 3e), this central low-resistivity zone begins to dissipate at around 300 m a.s.l. (Figure 3f).
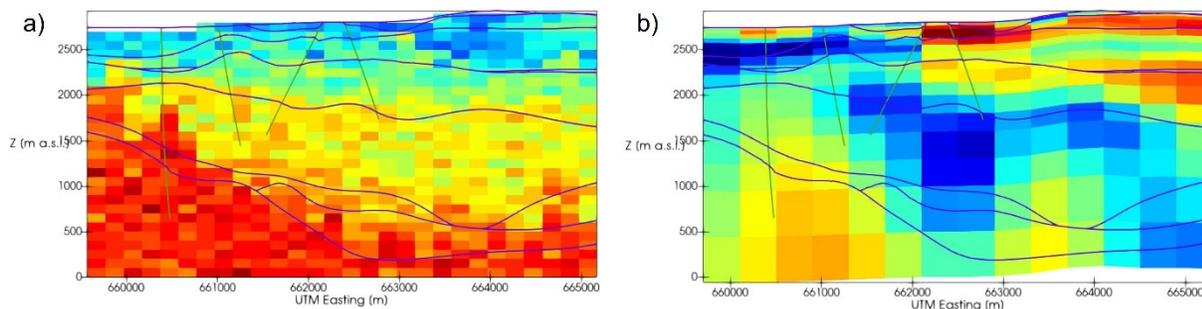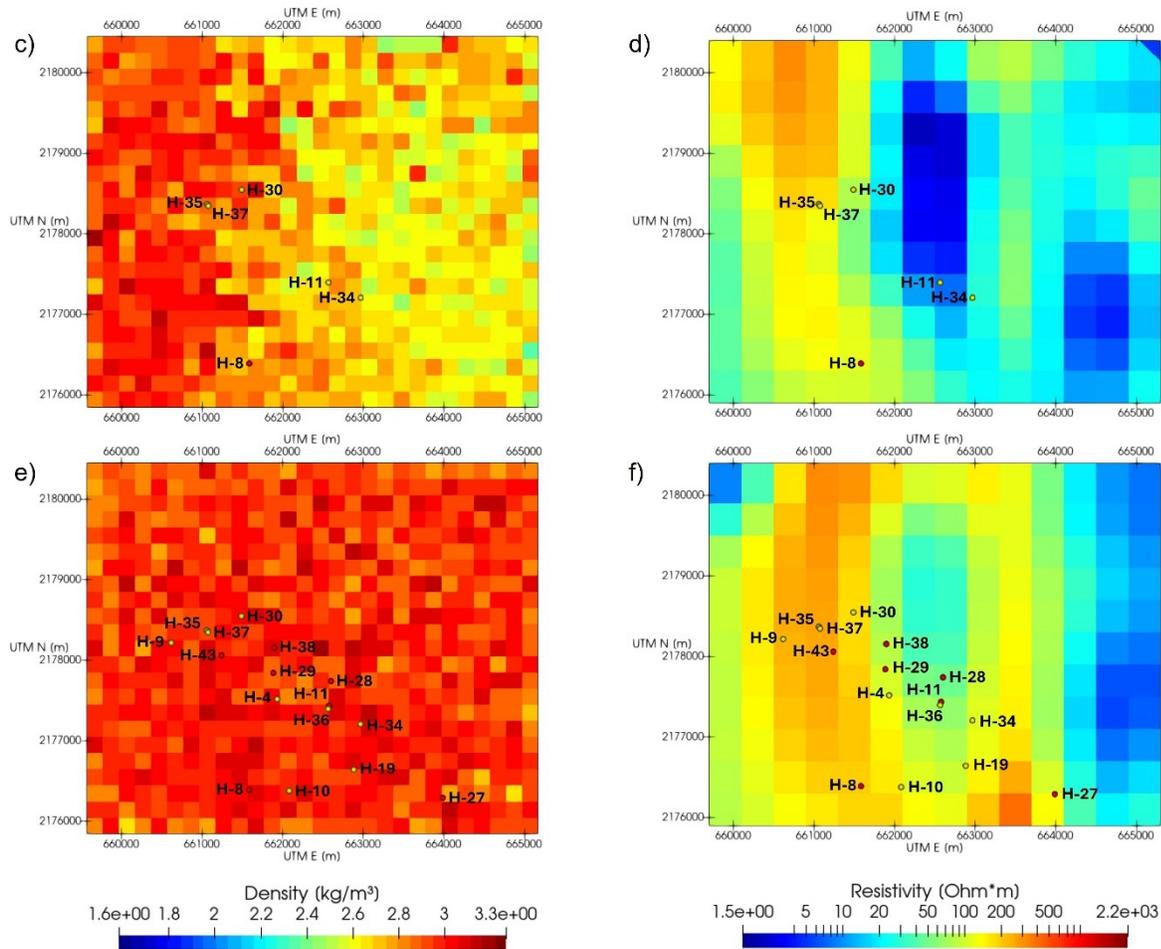
Figure 3: Vertical profiles through a) the gravity inversion model (Cornejo-Triviño et al., subm.) and b) the 3D electric resistivity inversion (Benediktsdóttir et al., 2019). Blue lines represent major geological boundaries, and black lines mark the fault traces, based on Calcagno et al. (2022). Top-view horizontal slices of c) density and (d) resistivity at 1,200 m a.s.l., and corresponding slices at 300 m a.s.l. in e) and f), respectively.

Although the spatial resolution of both gravity and magnetotelluric inversion data could, in principle, allow for the detection of deep anomalies, our current analysis indicates that neither method has clearly delineated the sub- to supercritical fluid zones in the Los Humeros geothermal field. The absence of a distinct geophysical signature that correlates with the geochemical and temperature indicators suggests that these fluids may not produce strong or coherent anomalies at the scales resolved by the current models.

However, NW–SE striking structural features, previously identified through a morpho-structural analysis and regional gravity data (Figure 4; Cornejo-Triviño et al. 2024), are likely to play a critical role in the formation and localization of these high-temperature fluids. The orientation of these structures is not only aligned with the zones of inferred sub- to supercritical conditions but have also been shown to influence the geometry and development of the Los Humeros caldera itself. Their persistent structural control across geological timescales suggests a deep-seated, tectonically driven mechanism that facilitates the ascent and accumulation of superheated fluids.

This reinforces the hypothesis that sub- to supercritical resources in Los Humeros are not simply controlled by lithological contrasts or shallow fault systems but rather are linked to long-lived regional tectonic structures that penetrate deep into the crust. Future exploration efforts may benefit from integrating this structural framework with high-resolution geophysical and geochemical data to more accurately target supercritical zones.
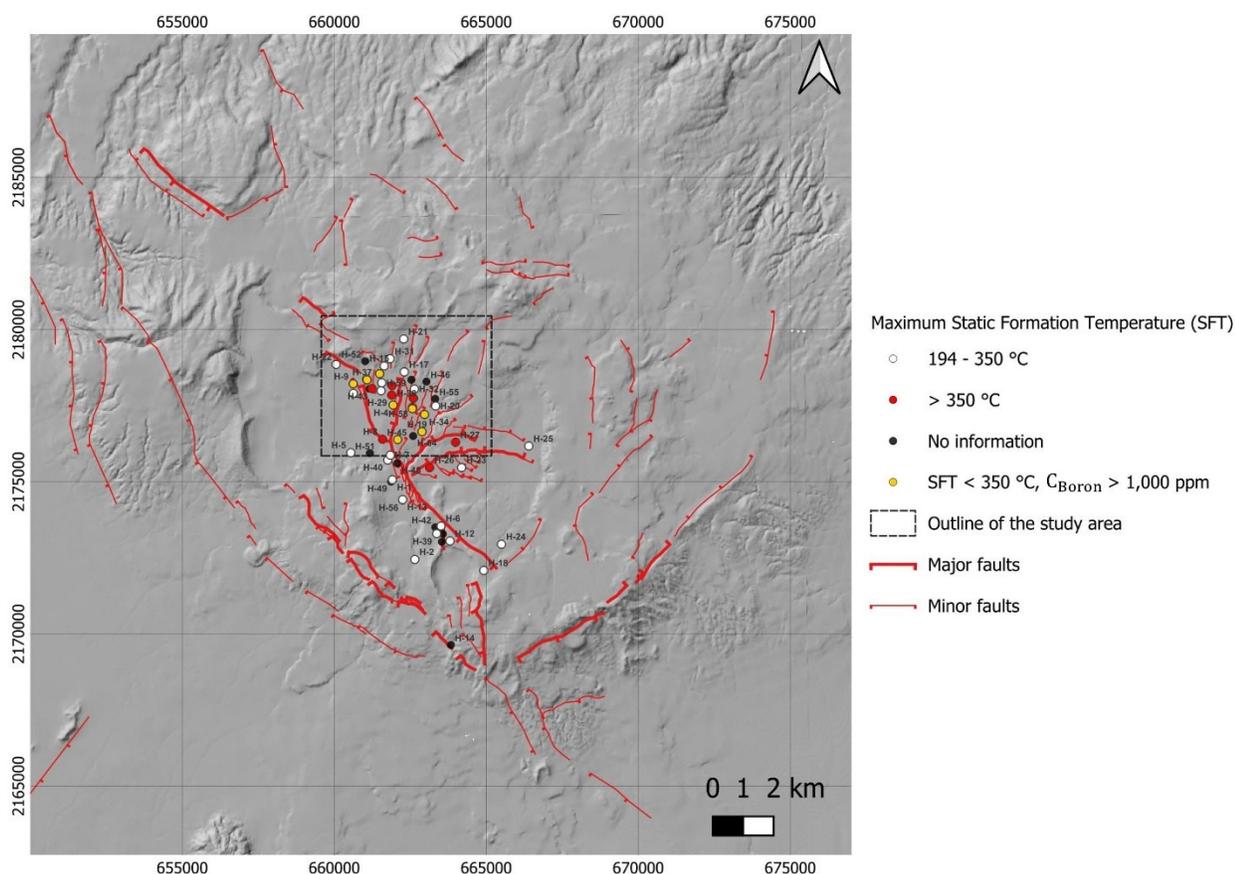
Figure 4: Distribution of wells and maximum static formation temperatures after Horner (1951) in the Los Humeros geothermal field (Espinosa-Paredes & Garcia-Gutierrez, 2003) or with mean boron concentrations C$_{Boron}$ > 1,000 ppm (data from Tello, 2005; Diez et al., 2015; Heřmanská et al., 2020). The black ellipsoids outline of the expected sub- to supercritical fluid extend based on the temperatures and confirmed by high boron concentrations. The faults have been identified by structural and remote sensing analyses (Cornejo-Triviño et al., 2024).

5. CONCLUSION

Sub- and supercritical geothermal systems represent one of the most promising frontiers in geothermal energy development, offering substantially higher energy densities than conventional hydrothermal resources. At the Los Humeros geothermal field, integrated analyses of temperature, fluid chemistry, gravity, and magnetotelluric data point toward the possible existence of sub- to supercritical conditions in the northern sector of the reservoir.

The spatial arrangement of wells with elevated temperatures and boron concentrations follows NE–SW trending structural corridors, and morpho-structural analyses highlight NW–SE striking faults as possible conduits. These structures likely play a central role in the ascent and localization of high-temperature fluids, indicating a tectonically driven system rather than one governed solely by local lithological variations.

Despite the high resolution of both gravity and magnetotelluric inversion models, neither clearly delineates the zones of elevated temperature and boron concentration. The lack of strong or coherent geophysical signatures at the resolved scales suggests the need for complementary datasets or refined approaches in interpretation and modeling.

Overall, these findings highlight both the potential and the diagnostic challenges associated with recognizing supercritical resources in active volcanic geothermal systems.

Schill et al.

REFERENCES

Benediktsdóttir, A., Hersir, G., Vilhalmsson, A., Manzella, A., Santilano, A., & Held, S. (2019). Report on resistivity modelling and comparison with other SHGS. Deliverable D.5.2, WP5.

Bernard, R. (2008). Isotopos de H, O, He, C and N en fluidos hidrotermales del Cinturon Volcanico Mexicano. [MS Thesis]. In Posgrado de Ciencias de la Tierra, UNAM, 157 pp).

Bernard, R., Taran, Y., Pennisi, M., Tello, E., & Ramirez, A. (2011). Chloride and Boron behavior in fluids of Los Humeros geothermal field (Mexico): A model based on the existence of deep acid brine. Applied Geochemistry, 26(12), 2064–2073. https://doi.org/10.1016/j.apgeochem.2011.07.004

Calcagno, P., Trumpy, E., Gutiérrez-Negrín, L. C., & Liotta, D. (2022). A collection of 3D geomodels of the Los Humeros and Acoculco geothermal systems (Mexico). Scientific Data, 9(1). https://doi.org/10.1038/s41597-022-01327-0

Carrasco-Núñez, G., Bernal, J. P., Dávila, P., Jicha, B., Giordano, G., & Hernández, J. (2018). Reappraisal of Los Humeros Volcanic Complex by New U/Th Zircon and 40 Ar/ 39 Ar Dating: Implications for Greater Geothermal Potential. Geochemistry, Geophysics, Geosystems, 19(1), 132–149. https://doi.org/10.1002/2017GC007044

Carrasco-Núñez, G., Cavazos-Álvarez, J., Dávila-Harris, P., Bonini, M., Giordano, G., Corbo-Camargo, F., Hernández, J., López, P., & Lucci, F. (2022). Assembly and development of large active calderas hosting geothermal systems: Insights from Los Humeros volcanic complex (Mexico). Journal of South American Earth Sciences, 120. https://doi.org/10.1016/j.jsames.2022.104056

Carrillo, J., Pérez-Flores, M. A., & Calò, M. (2024). Three-dimensional joint inversion of surface wave dispersion and gravity data using a petrophysical approach: an application to Los Humeros Geothermal Field. Geophysical Journal International, 239(2), 1217–1235. https://doi.org/10.1093/gji/ggae333

Cavazos-Álvarez, J. A., Carrasco-Núñez, G., Dávila-Harris, P., Peña, D., Jáquez, A., & Arteaga, D. (2020). Facies variations and permeability of ignimbrites in active geothermal systems; case study of the Xáltipan ignimbrite at Los Humeros Volcanic Complex. Journal of South American Earth Sciences, 104, 102810. https://doi.org/10.1016/j.jsames.2020.102810

Cornejo-Triviño, N., Liotta, D., Piccardi, L., Brogi, A., Kruszewski, M., Perez-Flores, M. A., Carrillo, J., Calcagno, P., Sass, I., & Schill, E. (2024). Gravimetric and morpho-structural analyses in the superhot geothermal system Los Humeros: an example from central Mexico. Geothermal Energy, 12(1). https://doi.org/10.1186/s40517-024-00285-7

Cornejo-Triviño, N., Weydt, L. M., Sass, I., & Schill, E. (n.d.). In-situ density and litho-constrained modeling of gravity data in the Los Humeros geothermal field, Mexico. Submitted for Publication. https://doi.org/10.21203/rs.3.rs-7538801/v1

Craig, H. (1961). Isotopic Variations in Meteoric Waters. Science, 133(3465), 1702–1703. https://doi.org/10.1126/science.133.3465.1702

Diez, H., Flores, M., Ramírez, M., Tovar, R., Rosales, C., Solano, F., & Sandoval, F. (2015). Neutralization of acid fluids from well H-43 (superheated steam), Los Humeros Geothermal Field, Mexico. World Geothermal Congress, 1–6.

Espinosa-Paredes, G., & Garcia-Gutierrez, A. (2003). Estimation of static formation temperatures in geothermal wells. Energy Conversion and Management, 44(8), 1343–1355. https://doi.org/10.1016/S0196-8904(02)00117-6

Heřmanská, M., Kleine, B. I., & Stefánsson, A. (2020). Geochemical constraints on supercritical fluids in geothermal systems. Journal of Volcanology and Geothermal Research, 394. https://doi.org/10.1016/j.jvolgeores.2020.106824

Hinojosa, E. T. (2005). Estado de equilibrio soluto-mineral y saturación de minerales de alteración en fluidos geotérmicos de alta temperatura de México. [Tesis doctoral]. Universidad Autónoma de México.

Horner, DR. (1951). Pressure build-up in wells. 3rd World Petroleum Congress, 503–522.

Lelli, M., Kretzschmar, T. G., Cabassi, J., Doveri, M., Sanchez-Avila, J. I., Gherardi, F., Magro, G., & Norelli, F. (2021). Fluid geochemistry of the Los Humeros geothermal field (LHGF - Puebla, Mexico): New constraints for the conceptual model. Geothermics, 90. https://doi.org/10.1016/j.geothermics.2020.101983

Martínez-Serrano, R. G. (2002). Chemical variations in hydrothermal minerals of the Los Humeros geothermal system, Mexico. Geothermics, 31(5), 579–612. https://doi.org/10.1016/S0375-6505(02)00015-9

Nono, F., Gibert, B., Parat, F., Loggia, D., Cichy, S. B., & Violay, M. (2020). Electrical conductivity of Icelandic deep geothermal reservoirs up to supercritical conditions: Insight from laboratory experiments. Journal of Volcanology and Geothermal Research, 391. https://doi.org/10.1016/j.jvolgeores.2018.04.021

Siripunvaraporn, W., & Egbert, G. (2009). WSINV3DMT: Vertical magnetic field transfer function inversion and parallel implementation. Physics of the Earth and Planetary Interiors, 173(3–4), 317–329. https://doi.org/10.1016/j.pepi.2009.01.013

Siripunvaraporn, W., Egbert, G., Lenbury, Y., & Uyeshima, M. (2005). Three-dimensional magnetotelluric inversion: data-space method. Physics of the Earth and Planetary Interiors, 150(1–3), 3–14. https://doi.org/10.1016/j.pepi.2004.08.023

Soyer, W., Mackie, R., Hallinan, S., Miorelli, F., & Siagian, H. (2020). 3D MT and Gravity Joint Inversion Modeling of Graben-Hosted High Temperature Geothermal Fields. 1st Geoscience & Engineering in Energy Transition Conference, 1–5. https://doi.org/10.3997/2214-4609.202021061

Tello, H. E. (2005). Estado de equilibrio soluto-mineral y saturación de minerales de alteración en fluidos geotérmicos de alta temperature. [Tesis doctoral, Universidad Autónoma de México]. https://tesiunamdocumentos.dgb.unam.mx/ptb2005/01190/0346539/0346539_A1.pdf

Um, E. S., Commer, M., Gritto, R., Peacock, J. R., Alumbaugh, D. L., Jarpe, S. P., & Hartline, C. (2023). Cooperative joint inversion of magnetotelluric and microseismic data for imaging the Geysers geothermal field, California, USA. Geophysics, 88(5), WB45–WB54. https://doi.org/10.1190/geo2022-0521.1

Yáñez-García, C., & García-Durán, S. (1982). Exploración de la región geotérmica Los Humeros-Las Derrumbadas, estados de Puebla y Veracruz (Report). Comision Federal de Electricidad, Mexico.